Superexcited State Dynamics Probed with an Extreme-Ultraviolet Free Electron Laser

Wen Li,[1,2] Robert R. Lucchese,[3] Adnan Doyuran,[4] Zilu Wu,[4] Henrik Loos,[4] Gregory E. Hall,[2] and Arthur G. Suits[1,2,*]

[1]*Department of Chemistry, Stony Brook University, Stony Brook, New York 11794, USA*
[2]*Chemistry Department, Brookhaven National Laboratory, Upton, New York 11973, USA*
[3]*Department of Chemistry, P.O. Box 30012, Texas A&M University, College Station, Texas 77842, USA*
[4]*National Synchrotron Light Source, Brookhaven National Laboratory, Upton, New York 11973, USA*

(Received 14 August 2003; published 27 February 2004)

We present the first experimental results obtained with a high-gain harmonic generation extreme ultraviolet free electron laser. The experiment probes decay dynamics of superexcited states of methyl fluoride via ion pair imaging spectroscopy. Velocity mapped ion images of the fluoride ion, obtained with excitation via intense, coherent, subpicosecond pulses of 86–89 nm radiation, reveal low translational energy, implying very high internal excitation in the methyl cation cofragment. Angular distributions show changing anisotropy as the excitation energy is tuned through this region. The dynamics underlying the dissociation are discussed with the aid of theoretical calculations.

DOI: 10.1103/PhysRevLett.92.083002 PACS numbers: 33.80.Rv, 33.80.Eh, 34.50.Gb, 41.60.Cr

Superexcited states are neutral molecular states embedded in the ionization continuum, and they contribute significantly to molecular photophysics in the extreme ultraviolet (XUV) region [1,2]. Ion pair states [3] represent one class of high-lying neutral states that have been used to probe superexcited state photoexcitation processes, notably in the work of Mitsuke and co-workers [4–8] and Eland *et al.* [9]. Hepburn and co-workers have recently used threshold excitation of these states, followed by dissociation in a weak Stark field, to obtain very high resolution measurements of the energies of these dissociation asymptotes [10–12]. Hikosaka and Eland have studied ion pair formation in methyl fluoride at 21 eV using coincidence detection [9]. They found evidence to support formation of electronically excited methyl cations as suggested by Mitsuke *et al.* [8]. In our laboratory, we have used ion pair imaging of methyl chloride to provide spectroscopic information on the methyl cation [13,14]; in that unusual case, the ion pair states actually lie below the ionization continuum. In this Letter we present results for ion pair dissociation of methyl fluoride around 14 eV using velocity mapped imaging of the F^- and CH_{3^+} product fragments. These are the first experimental applications of the extreme ultraviolet free electron laser (XUV-FEL) under development at Brookhaven National Laboratory (BNL), and the first results ever obtained with a high-gain harmonic generation based free electron laser.

Single-pass free electron laser sources in the XUV and x-ray wavelength region are currently the subject of intense interest and investigation, as the development of high power, coherent femtosecond pulses in this region will enable important new scientific opportunities in time-resolved dynamics and nonlinear photophysics [15]. The strategies for developing these future ''fourth-generation'' light sources are thus the subject of considerable discussion and debate. The XUV-FEL at BNL is one of several such sources currently under development, but is unique in that it relies on high-gain harmonic generation (HGHG) from a seed laser pulse, rather than self-amplified spontaneous emission (SASE) [16,17]. As a result, the radiation exhibits many of the desirable properties of the seed laser, providing better stability and control of the central wavelength and smaller energy fluctuations than SASE. One possible strategy for developing future x-ray FEL sources relies on cascaded stages of HGHG. A key question in this regard is the stability and reliability of the HGHG process; the present results speak directly to this issue.

The FEL source has been described in detail recently [17], but the relevant features are briefly repeated here. In HGHG, a small energy modulation is imposed on the electron beam by interaction with a seed laser in a short undulator; this is subsequently converted to a coherent longitudinal density modulation. In the second undulator (the radiator), tuned to the nth harmonic of the seed frequency, the microbunched electron beam emits coherent radiation at the harmonic frequency $n\omega$, which is then amplified until saturation. The FEL beam consists of the radiator fundamental at 266 nm (ca. 100 μJ/pulse, 600–800 fs) as well as its second and third harmonics, measured to be 0.1 and 0.3μJ/pulse), respectively. The bandwidth is 0.1% full-width at half maximum on the radiator fundamental at 266 nm.

The experimental end station is an ion imaging apparatus [18] with a multilens velocity mapping [19] ion optics system. The experiment employed a pulsed molecular beam source of 20% methyl fluoride in argon generated from a piezoelectric valve. The beam is skimmed before entering a separate interaction chamber where it is crossed at 90° by the FEL beam. The interaction occurs on the axis of a velocity-focusing time of flight mass spectrometer that is coupled to a 75 mm diameter imaging microchannelplate detector. The FEL

beam is linearly polarized perpendicular to the ion time of flight axis and parallel to the detector plane. The detector is viewed by a fast-scan charge-coupled device camera, and the images are read into a computer and integrated after applying real-time discrimination and centroiding of the product ion spots. The detected mass is selected by applying an appropriate gate pulse to the detector, and negative or positive ions are readily detected by applying the appropriate polarity to the ion optics.

Velocity mapped images of the fluoride ion are shown in Fig. 1 for photon energies of 13.52, 13.68, and 13.95 eV. The linearly polarized XUV radiation is vertical in the plane of the figure. These are two-dimensional projections of the recoiling F^- velocity distribution, and the three-dimensional distributions are recovered by Vrakking's iterative reconstruction technique [20]. The product translational energy and angular distributions are then obtained by the appropriate integration of the slice through the three-dimensional distribution.

The translational energy distributions are shown in Fig. 2(a) for all three photoexcitation energies. These distributions, showing an average total translational energy release of 0.31–0.32 eV, all peak near zero energy and are virtually indistinguishable. The dissociation energy of CH_3F to the separated ion pair is 11.33 eV, so that the measured translational energies account for only 12–14% of the available energy. The balance of the available energy must appear as internal energy of the methyl cation fragment. This partitioning of energy between translational and internal modes of the fragments can be compared to the statistical limit for a low angular momentum polyatomic molecule separating into an atom and a polyatomic fragment [21], in which the average translational energy would account for 17.6% of the available energy. The methyl cation fragments are somewhat hotter than this statistical limit.

The angular distributions, shown in Fig. 2(b), exhibit modest anisotropy, and this clearly changes from predominantly perpendicular at 13.52 eV to predominantly parallel at 13.95 eV. These are fitted to the expression $I(\theta) = 1 + \beta P_2(\cos\theta)$, where P_2 is the second Legendre polynomial and θ is the recoil angle with respect to the

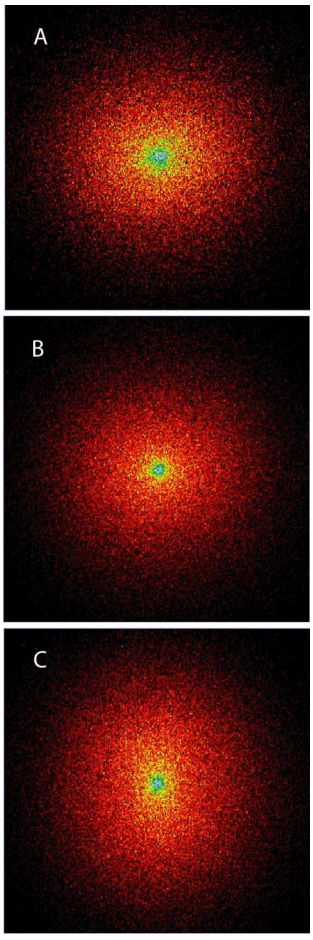

FIG. 1 (color online). F^- images from ion pair dissociation of methyl flouride at (a) 13.52 eV, (b) 13.68 eV, and (c) 13.95 eV photon energy.

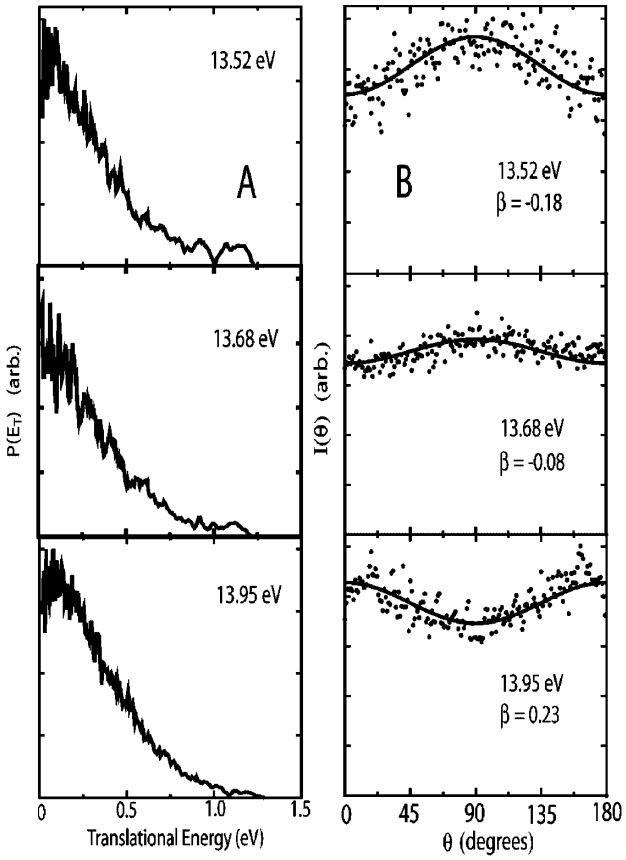

FIG. 2. (a) Total translational energy distributions obtained from images in Fig. 1 at the indicated photon energies. (b) F^- angular distributions from the images in Fig. 1. Points represent experimental results, the lines are fits obtained using the indicated values for β.

polarization vector of the XUV laser. The β parameters obtained from the images take the values shown in Fig. 2(b). In the energy range 13.5–14 eV, the photoabsorption spectrum of methyl fluoride shows a broad peak that has been assigned to excitation out of nearly degenerate $5a_1/1e$ valence orbitals to $3s$ and $3p$ Rydberg states [22]. These are the second highest occupied molecular orbitals (HOMO-1), and these Rydberg states thus converge to electronically excited states of the CH_3F cation. The ion pair excitation spectrum for methyl fluoride obtained by Mitsuke *et al.* actually has its onset in the region of this superexcited state: its appearance energy is about 12.4 eV, although the thermochemical threshold is fully 1 eV lower [8].

The value of β has also been estimated theoretically. Our theoretical model assumed that the ion pairs are formed by an initial excitation of a Rydberg level leading to the $5a_1^{-1}$ or $1e^{-1}$ hole states as indicated above. Then the computed β was determined by the relative strengths and polarizations of the transitions from the ground state to the Rydberg states. We computed the positions and oscillator strengths for these transitions using the improved virtual orbital (IVO) model [23]. We computed the IVO orbitals separately for each hole state using a cc-pVTZ basis set [24] which was augmented by two s, two p, and two d functions on the C and F atoms. The exponents were chosen to represent $n = 3$ Rydberg levels [25]. The IVO results for the transitions important for determining β in the range of energies in the experiment are given in Table I. These oscillator strengths and energies were then combined to yield a computed value of β. In the IVO approximation, the IPs are given by the Koopmans's theorem values, 18.35 eV for $5a_1^{-1}$ and 18.94 eV for $1e^{-1}$. These do not compare well with the experimental values which are 17.0 eV for both of these states [26]. To obtain a better estimate of the β's we have used theoretical values of the IPs that were computed using the Green's function (GF) method [26]. These values were 16.88 eV for $5a_1^{-1}$ and 17.19 eV for $1e^{-1}$. In the computation of β, we have distributed the oscillator strengths given in Table I using a Gaussian with full-width at half maximum of 1.0 eV, consistent with the anticipated Franck-Condon envelopes [26]. In Fig. 3 we have given the resulting β values. In the figure the dashed line is the computed values of β where we have allowed the IPs to vary and found the values that gave the best fit to the experiment. The optimal IPs were 16.87 eV for $5a_1^{-1}$ and 17.30 eV for $1e^{-1}$.

TABLE I. Results of IVO calculations. The values of transition energies are given relative to the corresponding Koopman's theorem IPs.

Transition	Polarization	Oscillator strength	IP-ΔE (eV)
$5a_1 \rightarrow 3s\,a_1$	Parallel	0.047	3.37
$5a_1 \rightarrow 3p\,a_1$	Parallel	0.225	2.81
$1e \rightarrow 3s\,a_1$	Perpendicular	0.404	3.63
$1e \rightarrow 3p\,a_1$	Perpendicular	0.015	3.14

The results of these computations indicate that both channels have a lower $3s\ a_1$ state and a higher $3p\ a_1$ state. In the case of the excitation from the $1e$ level, the strong excitation is to the lower of the two a_1 Rydberg states, whereas the higher energy excitation from the $5a_1$ level is the stronger of the two. The strong perpendicular excitation at lower energy combined with the strong parallel excitation at higher energy leads to the rising values of β as a function of photon energy seen in Fig. 3.

We now turn to a discussion of the ion pair dissociation dynamics, guided by schematic cuts through the CH_3F potential surfaces shown in Fig. 4. The dynamics of this dissociation begin with initial excitation to the superexcited $(5a_1/1e)^{-1}$ Rydberg states converging to excited states of the parent ion. The evidence for this is the close parallel between this band in the absorption spectrum and the ion pair excitation spectrum, as well as the F^- angular distributions discussed above. Internal conversion to highly vibrationally excited levels of the $2e^{-1}$ states follows on a subpicosecond time scale, with prompt dissociation of these states via direct coupling to the ion pair surfaces. Evidence for this is the very low translational energy release in the products. Direct coupling of the $(5a_1/1e)^{-1}$ Rydberg states to the ion pair surface would be expected to result in much lower internal energy in the CH_{3^+} and much larger translational energy release. The reason that access to the ion pair states does not occur directly from the $2e^{-1}$ manifold of Rydberg states is likely that, at these energies, Franck-Condon factors for

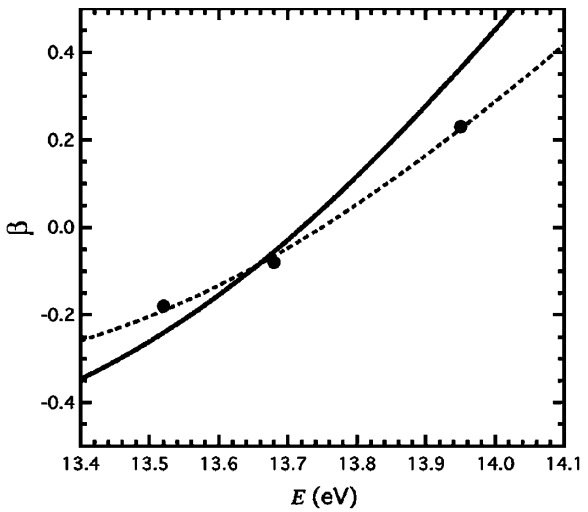

FIG. 3. Computed values of β (lines) compared to measured values (points). The solid line corresponds to the calculation using the GF values of the $5a_1^{-1}$ and $1e^{-1}$ IPs. The dashed line was obtained with the optimized values of the IPs.

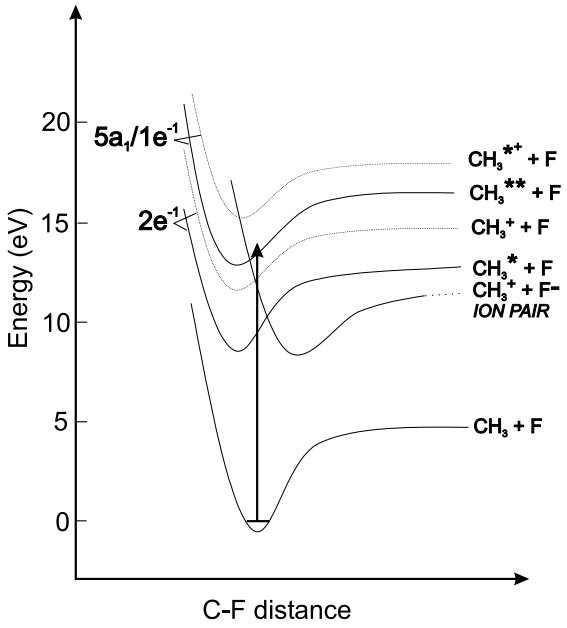

FIG. 4. Schematic cuts through relevant potential energy surfaces for methyl fluoride.

these transitions favor direct ionization. At lower energies, access to the ion pair surface from the $2e^{-1}$ Rydberg states may be obstructed by the barrier between the inner and outer wells shown in Fig. 4, or simply by inefficient coupling between these surfaces.

These studies, the first to be performed with an HGHG FEL, take advantage only of the intensity, narrow bandwidth, stability, and pulsed nature of the source. Other opportunities exist for future experiments to exploit the coherence and short pulse duration as well. This work, showing the detailed dynamics of superexcited state decay to ion pair products, clearly demonstrates the feasibility of performing complex studies using a laser seeded FEL.

We wish to thank D. Hanson for the use of the experimental chamber, and X. J. Wang, J. B. Murphy, L. H. Yu, S. Dierker, and the staff of the Source Development Laboratory at BNL for their support. This work was performed at Brookhaven National Laboratory under Contract No. DE-AC02-98CH10886 with the U.S. Department of Energy. A. G. S. acknowledges the support of the National Science Foundation under Grant No. CHE-0102174. R. R. L. acknowledges the support of the Robert A. Welch Foundation (Houston, TX) under Grant No. A-1020.

*Permanent address: Department of Chemistry, Wayne State University, Detroit, MI 48202, USA.
Electronic address: asuits@chem.wayne.edu

[1] J. Berkowitz, *Photoabsorption, Photoionization and Photoelectron Spectroscopy* (Academic Press, New York, 1979).
[2] Y. Hatano, J. Electron Spectrosc. Relat. Phenom. **119**, 107 (2001).
[3] J. Berkowitz, in *VUV and Soft x-Ray Photoionisation*, edited by U. Becker and D. A. Shirley (Plenum, New York, 1996), p. 263.
[4] K. Mitsuke, S. Suzuki, T. Imamura, and I. Koyano, J. Chem. Phys. **93**, 8717 (1990).
[5] K. Mitsuke, S. Suzuki, T. Imamura, and I. Koyano, J. Chem. Phys. **93**, 1710 (1990).
[6] K. Mitsuke, S. Suzuki, T. Imamura, and I. Koyano, J. Chem. Phys. **94**, 6003 (1991).
[7] K. Mitsuke, S. Suzuki, T. Imamura, and I. Koyano, J. Chem. Phys. **95**, 2398 (1991).
[8] S. Suzuki, K. Mitsuke, T. Imamura, and I. Koyano, J. Chem. Phys. **96**, 7500 (1992).
[9] Y. Hikosaka and J. H. D. Eland, Rapid Commun. Mass Spectrom. **14**, 2305 (2000).
[10] J. D. D. Martin and J.W. Hepburn, Phys. Rev. Lett. **79**, 3154 (1997).
[11] J. D. D. Martin and J.W. Hepburn, J. Chem. Phys. **109**, 8139 (1998).
[12] R. C. Shiell, X. K. Hu, Q. C. J. Hu, and J.W. Hepburn, Faraday Discuss. **115**, 331 (2000).
[13] M. Ahmed, D. S. Peterka, P. Regan, X. H. Liu, and A. G. Suits, Chem. Phys. Lett. **339**, 203 (2001).
[14] X. H. Liu, R. L. Gross, and A. G. Suits, Science **294**, 2527 (2001).
[15] H. Wabnitz *et al.*, Nature (London) **420**, 482 (2002).
[16] L.-H. Yu *et al.*, Science **289**, 932 (2000).
[17] A. Doyuran *et al.*, Phys. Rev. Lett. **86**, 5902 (2001).
[18] D. Chandler and P. Houston, J. Chem. Phys. **87**, 1445 (1987).
[19] A. Eppink and D. Parker, Rev. Sci. Instrum. **68**, 3477 (1997).
[20] M. J. J. Vrakking, Rev. Sci. Instrum. **72**, 4084 (2001).
[21] J. T. Muckerman, J. Phys. Chem. **93**, 179 (1989).
[22] R. Locht, B. Leyh, A. Hoxha, H. J. D. Dehareng, and H. Baumgartel, Chem. Phys. **257**, 283 (2000).
[23] W. Hunt and I.W. A. Goddard, Chem. Phys. Lett. **3**, 414 (1969).
[24] T. H. Dunning, Jr., J. Chem. Phys. **90** 1007(1989).
[25] T. H. Dunning, Jr. and P. J. Hay, in *Methods of Electronic Structure Theory*, edited by H. F. Schaefer (Plenum Press, New York, 1977).
[26] G. Bieri, L. Asbrink, and W. von Niessen, J. Electron Spectrosc. Relat. Phenom. **23**, 281 (1981).